

## Fabrication of nanostructures of polyethylene glycol for applications to protein adsorption and cell adhesion

This content has been downloaded from IOPscience. Please scroll down to see the full text.

2005 Nanotechnology 16 2420

(<http://iopscience.iop.org/0957-4484/16/10/072>)

View [the table of contents for this issue](#), or go to the [journal homepage](#) for more

Download details:

IP Address: 18.7.29.240

This content was downloaded on 25/05/2014 at 19:18

Please note that [terms and conditions apply](#).

# Fabrication of nanostructures of polyethylene glycol for applications to protein adsorption and cell adhesion

P Kim<sup>1</sup>, D H Kim<sup>2</sup>, B Kim<sup>3</sup>, S K Choi<sup>4</sup>, S H Lee<sup>4</sup>,  
A Khademhosseini<sup>5</sup>, R Langer<sup>5</sup> and K Y Suh<sup>1,6</sup>

<sup>1</sup> School of Mechanical and Aerospace Engineering, Seoul National University, Seoul 151-742, Korea

<sup>2</sup> Microsystem Research Center, Korea Institute of Science and Technology, Seoul 138-791, Korea

<sup>3</sup> School of Aerospace and Mechanical Engineering, Hankuk Aviation University, Kyonggi-do 412-791, Korea

<sup>4</sup> School of Life Sciences and Biotechnology, Korea University, Seoul 136-701, Korea

<sup>5</sup> Harvard-MIT Division of Health Science and Technology, Massachusetts Institute of Technology, Cambridge, MA 02139, USA

E-mail: [sky4u@snu.ac.kr](mailto:sky4u@snu.ac.kr)

Received 10 June 2005, in final form 19 July 2005

Published 2 September 2005

Online at [stacks.iop.org/Nano/16/2420](http://stacks.iop.org/Nano/16/2420)

## Abstract

A simple method was developed to fabricate polyethylene glycol (PEG) nanostructures using capillary lithography mediated by ultraviolet (UV) exposure. Acrylate-containing PEG monomers, such as PEG dimethacrylate (PEG-DMA, MW = 330), were photo-cross-linked under UV exposure to generate patterned structures. In comparison to unpatterned PEG films, hydrophobicity of PEG nanostructure modified surfaces was significantly enhanced. This could be attributed to trapped air in the nanostructures as supported by water contact angle measurements. Proteins (fibronectin, immunoglobulin, and albumin) and cells (fibroblasts and P19 EC cells) were examined on the modified surfaces to test for the level of protein adsorption and cell adhesion. It was found that proteins and cells preferred to adhere on nanostructured PEG surfaces in comparison to unpatterned PEG films; however, this level of adhesion was significantly lower than that of glass controls. These results suggest that capillary lithography can be used to fabricate PEG nanostructures capable of modifying protein and cell adhesive properties of surfaces.

(Some figures in this article are in colour only in the electronic version)

## 1. Introduction

Polyethylene-glycol- (PEG-) based polymers are of great importance as biomaterials for applications in cell and tissue engineering, coating of implants, biosensors, and drug delivery systems [1, 2]. In particular, PEG coatings have been used to minimize surface biofouling of plasma proteins and to create surfaces that are invisible to cells. Recently,

PEG patterned substrates have been constructed to generate patterns of proteins or cells using microcontact printing [3–5], membrane lift-off [6, 7], microfluidic networking [8], and photolithography [9–11]. In these applications, PEG-based polymers control adsorption of proteins and adhesion of cells. Thus, the fabrication of a PEG surface capable of modifying protein and cell adhesive properties would be potentially of benefit.

We have previously fabricated PEG-based microstructures using moulding and dewetting techniques [12–14]. These

<sup>6</sup> Author to whom any correspondence should be addressed.

methods utilize capillary forces in the course of pattern formation, and are therefore referred to as capillary lithography. Using the protein and cell resistant properties of PEG, micropatterns were fabricated on oxide-based substrates (e.g., glass and silicon oxides) with precise control over surface topography and surface chemistry [14].

Nanofabrication of PEG hydrogels, however, is difficult due to limited availability and difficulty in fabrication of high aspect ratio sub-100 nm moulds. This is because high aspect ratio poly(dimethyl siloxane) (PDMS) moulds with nanostructure features are difficult to obtain due to the low elastic modulus of PDMS ( $\sim 1.8$  MPa). In addition, the high compressibility of PDMS ( $\sim 2.0$  N mm $^{-2}$  for Sylgard 184) gives rise to deformation, buckling, or collapse of shallow relief features [15, 16] and high surface tension, which causes rounding of sharp corners when released from the master [17]. These mechanical shortcomings of PDMS are currently limiting the successful replication and generation of features below a few hundred nanometres. Photolithographic patterning of PEG hydrogels is an alternative route to microfabrication [9–11]; however, the resolution of this technique is a few hundred nanometres as well.

Recently, ultraviolet (UV) curable moulds made from polyurethane functionalized with acrylate groups have been introduced to replace the PDMS mould for sub-100 nm lithography [18–20]. The backbone of the cured mould is poly(urethane acrylate) (PUA) and thus the moulding process is referred to as PUA moulding.

Herein, we introduce a simple, convenient method to nanofabricate PEG hydrogels without the use of photo-masks or PDMS moulds. PUA moulds were used to generate features as small as 50 nm using a photo-cross-linkable PEG dimethacrylate (PEG-DMA, MW = 330). In order to ease the release of the moulds from the substrate, PUA moulds were treated with a 1% amorphous fluoropolymer in tetrafluoroethylene (TFE) prior to mould placement. A number of proteins (fibronectin, immunoglobulin, and albumin) and cells (fibroblast and P19 EC cell) were tested to measure the relative adhesion amount of proteins and cells on nanostructure surfaces. Protein adsorption or cell adhesion was increased on PEG nanostructures, presumably due to changes in the wettability of the substrate and increased surface area. With its ease of use and superior performance, this approach could potentially be beneficial for various nanoprinting and nanofabrication approaches.

## 2. Materials and methods

### 2.1. Materials

UV curable polyurethane functionalized with acrylate groups was kindly provided by Minuta Tech. (MINS101m, Korea). All tissue culture media and serum were purchased from Gibco Invitrogen Corporation, cell lines were purchased from the American Tissue Type Collection and all chemicals were purchased from Aldrich-Sigma, unless otherwise indicated.

### 2.2. Fabrication of UV curable moulds

UV curable PUA moulds were comprised of polyurethane prepolymers, a monomeric modulator, photoinitiator and a

radiation curable releasing agent. Details on the synthesis and characterization of the polymer have been published elsewhere [19]. Various PUA moulds were tested with features ranging from 150 nm dots to lines with sizes from 50 to 200 nm. For protein adsorption and cell adhesion studies, the moulds had negative features (sticking in) with a lateral dimension of  $\sim 150$  nm at base and  $\sim 50$  nm at top and with a height ranging from  $\sim 300$  to  $\sim 500$  nm.

### 2.3. Fabrication of PEG-DMA nanostructures

Glass or silicon was used as the substrate for nanopatterning. Prior to application of the PUA mould, the substrate was thoroughly rinsed with ethanol to remove excess organic molecules and dried in a stream of nitrogen. A small amount of pure PEG-DMA (50–200  $\mu$ l) was drop-dispensed on the substrate and the PUA mould was carefully placed on top of the surface to make conformal contact. To cure, the sample was exposed to UV ( $\lambda = 250$ – $400$  nm) for a few minutes through the transparent backplane (dose = 100 mJ cm $^{-2}$ ) after adding 0.5 wt% of the UV initiator (2,2-dimethoxy-2-phenylacetophenone, Aldrich) with respect to the amount of polymer. After the UV curing, the mould was peeled off. To prevent delamination of the cured PEG nanostructure from the surface, the PUA mould was treated with a 1% amorphous fluoropolymer (Dupont Teflon AF 2400) in tetrafluoroethylene (TFE) prior to mould placement [21]. The Dupont Teflon AF 2400 is a copolymer of 2,2-bistrifluoromethyl-4,5-difluoro-1,3-dioxole (PDD) and tetrafluoroethylene. The non-reactivity/inertness nature with a low surface energy of 15.6 dyn cm $^{-1}$  (PDMS  $\sim 19.6$  dyn cm $^{-1}$ ) makes it possible to cleanly remove the mould (or de-moulding) from the patterned PEG structure without any mould surface treatment and without deterioration in surface properties over many patterning cycles.

### 2.4. Contact angle measurements

Static contact angles were measured with a Ramé–Hart goniometer (Mountain Lakes) equipped with a video camera. Reported values represent averages of at least six independent measurements.

### 2.5. Protein adsorption

Rhodamine-labelled bovine serum albumin (BSA), rhodamine-labelled IgG and fibronectin (FN) (Sigma) were dissolved in phosphate-buffered saline (PBS) (Sigma) at 50, 50 and 20  $\mu$ g ml $^{-1}$ , respectively. To test for BSA and IgG protein adhesion, a few drops of the protein solution was evenly distributed onto the surfaces and stored at room temperature for 30 min. The samples were then washed and directly analysed under a fluorescent microscope (Axiovert 200, Zeiss). To coat with FN, surfaces were dipped into a solution containing FN for 15 min. To measure FN adhesion, the surfaces were stained with anti-FN antibody (Sigma) for an additional 45 min, followed by 1 h incubation with the rhodamine-labelled anti-rabbit secondary antibody. The surfaces were then washed with water and analysed. Fluorescent images were quantified using Scion Image software. Pixel intensities were averaged

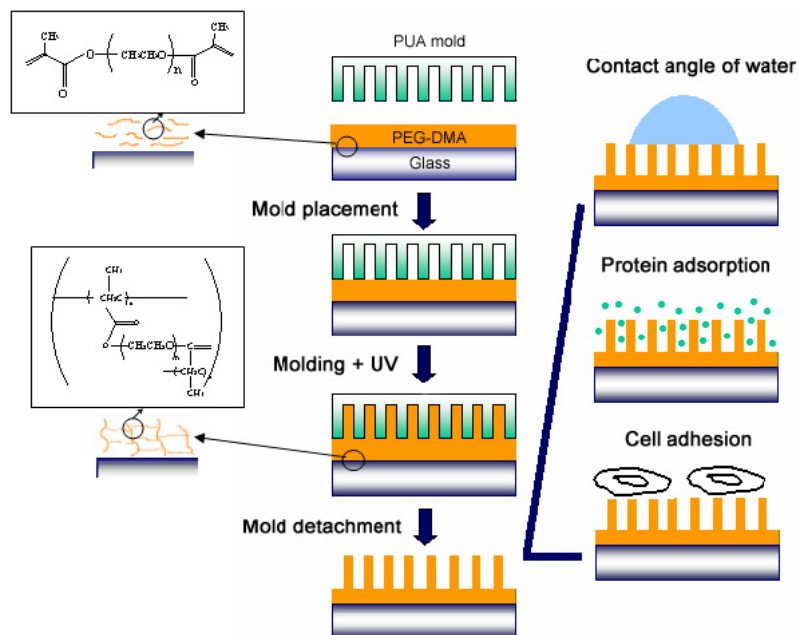


**Figure 1.** A schematic diagram of the experimental procedure. Initially, a uniform PEG-DMA film is prepared by drop dispensing followed by the placement of a PUA mould and then patterned by capillary lithography mediated by UV cross-linking. Some PEG nanostructures were subsequently analysed by contact angle, protein adsorption, and cell adhesion measurements.

for more than five spots for at least two independent experiments. Unstained glass slides that were analysed at same exposure were used as negative controls.

## 2.6. Cell cultures

P19 EC cells were maintained in  $\alpha$ -MEM containing 10% heat-inactivated foetal bovine serum (FBS),  $50 \mu\text{g ml}^{-1}$  streptomycin, and  $50 \mu\text{g ml}^{-1}$  penicillin at  $37^\circ\text{C}$  in 5%  $\text{CO}_2$ . Cells were subcultured at 48 h intervals in order to maintain continuous exponential proliferation. To subculture, the medium was aspirated prior to washing cells in PBS (pH 7.0) and replaced with trypsin-EDTA consisting of 0.04% (W/V) EDTA and 0.025% (W/V) trypsin in PBS to dissociate cells individually. Following incubation at  $37^\circ\text{C}$  for 3 min, cells were dispersed into a single-cell solution. Subsequently, the cells were seeded at a concentration of  $\sim 10^4$  cells  $\text{cm}^{-2}$  on collagen-coated or non-treated surfaces.

Primary heart fibroblasts of neonatal rats (day 1, from Sprague–Dawley–Ivanovas) were isolated as previously described [22]. Briefly, fibroblasts that adhered on a tissue culture dish after a 1 h incubation in completed medium were trypsinized and subsequently cultured on collagen-coated nanopatterns or cover-glasses in Dulbecco's modified Eagle's medium (DMEM) (Gibco Invitrogen, Grand Island, NY, USA) containing 10% foetal bovine serum (Sigma),  $50 \mu\text{g ml}^{-1}$  streptomycin,  $50 \mu\text{g ml}^{-1}$  penicillin (Gibco Invitrogen) at  $37^\circ\text{C}$  in 5%  $\text{CO}_2$ .

## 2.7. Nuclear staining

To stain cells, P19 EC cells were fixed in 4% paraformaldehyde in PBS (pH 7.4) for 30 min. After fixation, the cells were washed in distilled water and stained with haematoxylin to

visualize nuclei. The number of cells was counted under a phase-contrast microscope (TE2000-U, Nikon Co, Japan). Images were recorded by a digital camera (COOLPIX990, Nikon).

## 2.8. Environmental scanning electron microscopy (ESEM)

Morphological features, such as cell growth and adhesion, were examined using a field emission ESEM (FEI XL-30 FEG, Philips). Cultured cells were washed with phosphate-buffered saline (PBS, pH 7.4, Gibco Invitrogen) and fixed in 4% (W/V) paraformaldehyde (Sigma) in PBS for 30 min. After repeated washing in PBS, the cells were dehydrated in ethanol.

## 3. Results and discussion

### 3.1. Fabrication of PEG-DMA nanostructures

To pattern the substrates a thin film of the PEG polymer was formed by dispensing a few drops of the polymer on the substrate (figure 1). A PUA mould was then placed on the surface, forming a conformal contact with the surface. PEG-DMA in contact with the void spaces of the mould spontaneously moved into the PUA mould cavities by means of capillary action. The PEG structures were subsequently cured by exposure to UV for several minutes (figure 1). In contrast to PDMS moulds in which PEG structures maintained their physical integrity after the mould was removed, the PEG nanostructures formed using PUA moulds often stuck to the moulds after cross-linking and were subsequently removed from the surface. In order to solve this delaminating difficulty a flexible and transparent PET film was used, as reported previously [19, 20]. In addition, treating the surface of PUA moulds with a fluoropolymer was also observed to decrease its adhesive properties towards cross-linked PEG.

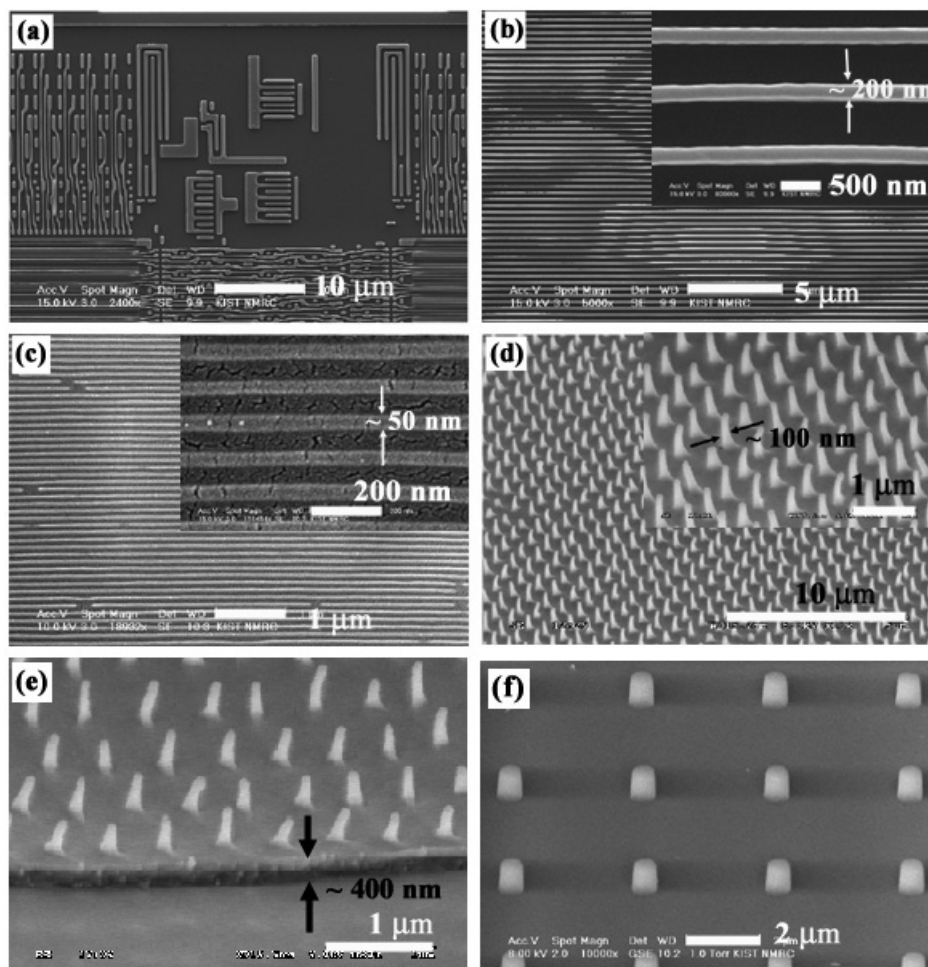


**Figure 2.** Various PEG nanostructures that formed on glass or silicon substrate: (a) a mixture of complicated patterns with the minimum line width of 80 nm, (b) 200 nm lines, (c) 50 nm lines, (d) 100 nm dots, (e) 100 nm dots at the edge showing a residual layer of  $\sim 400$  nm, and (f) 700 nm dots.

Figure 2 shows well defined nanofabricated PEG structures on glass or silicon substrates. Nanostructures were fabricated with various shapes including a complex structure (a) and lines with widths ranging from 200 nm (b) to 50 nm (c). Also dots of 100 nm ((d), (e)) and 700 nm (f) in diameter are shown in the figure with good pattern fidelity. The drop dispensing method of forming the layers resulted in a thick residual layer after the moulding process ( $>300$  nm) which is shown in figure 2(e). Although spin-coated PEG coatings did not form the thick residual layers, they resulted in air bubbles being trapped when the mould was placed on the surface, so care should be taken to decrease the thickness of the residual layer. For potential use as a lithographic resist, this problem needs to be addressed.

A direct application of the PEG nanostructures presented in this study is for protein and cell adhesion. PEG has a number of advantages in terms of cell adhesion [1, 2], which include its biocompatibility, allowing for minimal cell toxicity during long-term cell culture. In addition, PEG surfaces repel protein adhesion and subsequent formation of focal adhesions on these surfaces for cell attachment. This would substantially reduce time and effort to examine the underlying mechanism for cellular interactions with a nanotopography. Therefore,

the nanostructured PEG surface presented here would provide an efficient platform for studying the relation between the adhesion and growth of a certain cell type in the presence of nanotopographical features.

For protein adsorption and cell adhesion studies, we used PEG nanopillars as shown in figure 3(a) where the surface consists of two regions: the boxed PEG surface with a high density of nanopillars ( $\sim 150$  nm width at base and  $\sim 500$  nm space) and the blank PEG layer covering the rest of the surface. Figure 3(b) indicates that the nanopillars were formed on the entire surface with minimal defects, enabling a large-area process in one step. The height of the pillar was relatively uniform, ranging from 250 to 300 nm. These PEG nanostructures were robust and remained stable upon exposure to solvents such as water and ethanol for at least two weeks.

### 3.2. Contact angle of water on PEG-DMA nanostructures

To test for the changes in the hydrophobicity of the PEG nanostructured surfaces, we measured the contact angle of water on a glass slide, a bare PEG surface, and a PEG surface with nanopillars, respectively. The contact angle was  $20^{\circ}$ – $25^{\circ}$  on the bare PEG film and less than  $10^{\circ}$  on the glass. In contrast,

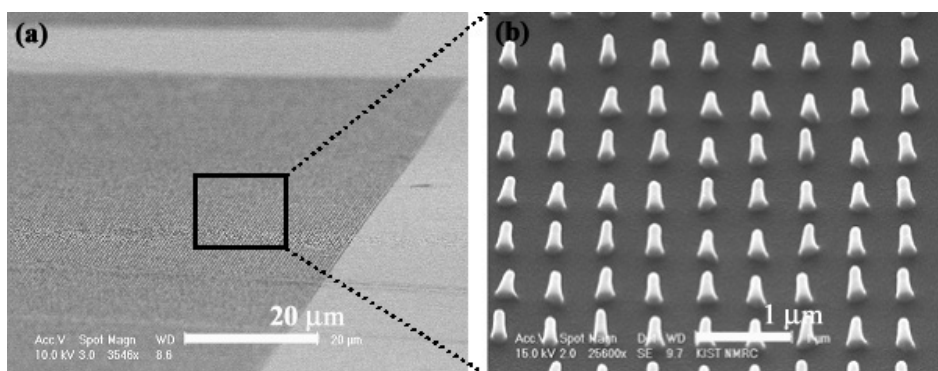


**Figure 3.** SEM images of uniform PEG nanopillars for protein adsorption and cell adhesion study: (a) a large area view showing both patterned dark (box) and non-patterned light regions and (b) a magnified view of individual nanopillars within the boxed area. The diameter of a nanopillar is about 150 nm at base and about 50 nm at top and aspect ratio is about 2.

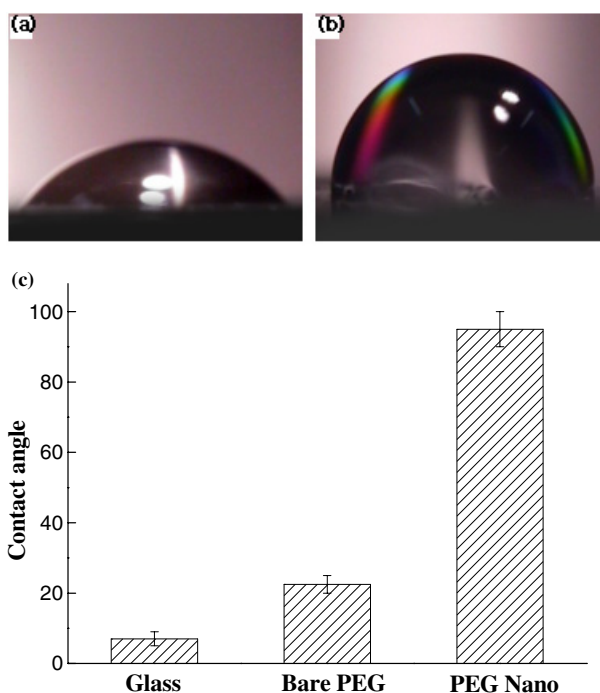
the contact angle was drastically increased to  $90^{\circ}$ – $100^{\circ}$ , changing the surface from hydrophilic to hydrophobic when a water drop is placed on the nanostructured surface of figure 3. The results are summarized in figure 4. It is anticipated that the air pocket in the spaces between the nanopillars is probably responsible for the hydrophobic nature of the PEG nanostructures (so called ‘Cassie state’) [23]. Although we did not carry out experiments on various nanostructures having different shapes and thus amounts of captured air, the measured contact angle on the PEG nanostructure seems to agree qualitatively with that predicted from theory. The relation between the contact angle of a flat surface  $\theta$  and that of a nanostructured surface  $\theta_1$  is given by [24]

$$\cos \theta_1 = f_1 \cos \theta - f_2 \quad (1)$$

where  $f_1$  and  $f_2$  are the fractional interfacial areas of the PEG nanopillars and of the air in the troughs between individual nanopillars, respectively (i.e.,  $f_1 + f_2 = 1$ ). It follows that  $\theta_1$  increases with increasing fraction of air,  $f_2$ . That is, an increase in the surface air fraction will enhance the water contact angle. If we put  $f_1 = 0.07$ ,  $f_2 = 0.93$ , and  $\theta = 22.5^{\circ}$  based on the geometry used here, we obtain  $\theta_1 \approx 149^{\circ}$ , much larger than the measured value ( $\theta_1 \sim 95^{\circ}$ ), in part due to the swelling of the PEG nanostructures. It is envisioned that changing the surface properties from hydrophilic to hydrophobic could be useful for various applications including smart microfluidic valves, and controlled drug release [25].

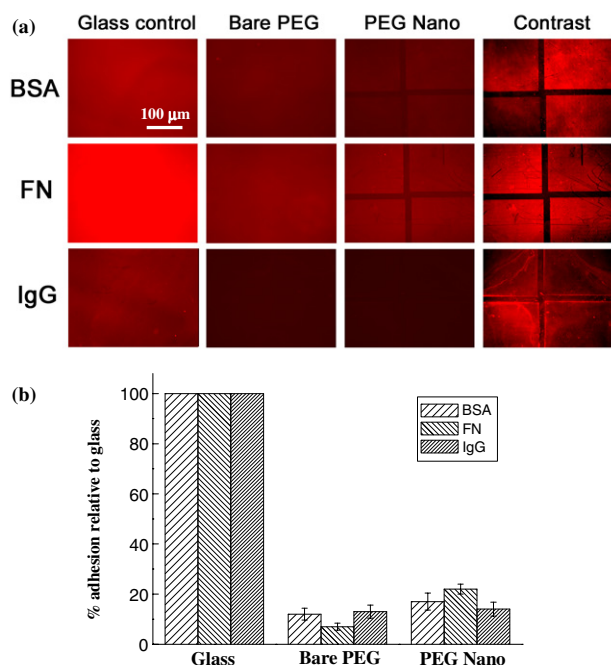
### 3.3. Protein adsorption on PEG-DMA nanostructures

Figure 5 shows the adsorption of three selected proteins: rhodamine-labelled albumin (BSA), fibronectin (FN), and rhodamine-labelled immunoglobulin (IgG) on glass, bare PEG (non-patterned), and PEG nanostructure, respectively. As shown in the figure, proteins adhered on the nanostructure surfaces in slightly higher amounts than on bare PEG surfaces, but less than on glass controls. This is because the relative amount of protein that is adsorbed on the surface is proportional to the surface area. According to a recent report [26], the fluorescent intensity from polymethyl methacrylate (PMMA) nanopillars formed by nanoimprint lithography was 2.3 times stronger than that of the flat area, suggesting that the increase



**Figure 4.** Measurements of the contact angle of water on (a) a bare PEG surface ( $\sim 22.5^{\circ}$ ) and (b) a PEG nanostructure ( $\sim 95^{\circ}$ ). (c) Contact angles on the three different surfaces.

of surface area is responsible for the behaviour. In our experiments, the intensity was increased to 1.2–3 times that of the bare PEG surface, depending on which protein was used, which also agrees with the increase of surface area qualitatively. In addition to the increase in surface area, the adsorption sites would be different on the surface as affected by a nanotopography. Recently, we observed that the amount of protein adhered on the tip of nanostructure is higher than that on the valley, suggesting that the surface energy would be different along the surface nanotopography. In the case of a heterogeneous surface consisting of different materials, the increase of protein adsorption by a factor of 2.5 was observed by increasing the effective surface only by 7% on the surface consisting of the flat and nanopyramidal surfaces using germanium islands on silicon [27].



**Figure 5.** (a) Fluorescent micrographs of rhodamine-BSA, FN and rhodamine-IgG on the surfaces of glass, bare PEG and PEG nanostructure (contrast enhancement included). The nanostructures are located within the boxes. (b) The graph summarizes the protein adsorption on the three different surfaces. The intensities were normalized using the glass control (100%). Note that the intensity was slightly increased on the nanostructure 1.2–3-fold depending on the type of protein.

### 3.4. Cell adhesion on PEG-DMA nanostructures

To examine whether an undifferentiated embryonic cell and a fibroblast behave differently on nanostructured substrates, we used P19 EC cells and primary heart fibroblasts of neonatal rats. As with protein adsorption, P19 EC cells or fibroblasts were seeded on glass, bare PEG (non-patterned) and PEG nanostructure, respectively, with or without collagen treatment. In the presence of collagen, the adhesion of P19 EC cells was slightly increased. As shown in figure 6, cell adhesion on the three surfaces was different on various surfaces after 2 days of culture. Interestingly, the number of adhered cells was increased on the nanostructure by more than threefold (25–27%) than that on the bare PEG surface (7–8%), but much less than that on the glass control (100%). Fibroblast showed no remarkable difference from P19 EC cells in adhesion (data not shown).

We postulate that the increased cell adhesion might have to do with the enhanced protein adsorption on the PEG nanopillars. In our experiment, protein adsorption was increased to 1.2–3 times that of the bare PEG surface, which would in turn lead to the increased cell adhesion. We further hypothesize that the change of focal adhesion sites would play a role in the increase of cell adhesion since we also observed an enhanced cell adhesion without collagen treatment. A recent report demonstrated that by culturing fibroblasts within defined nanostructures prepared by colloidal lithography a decrease in cytoskeletal organization and subsequent growth was observed [28, 29]. It was assumed that the reduced

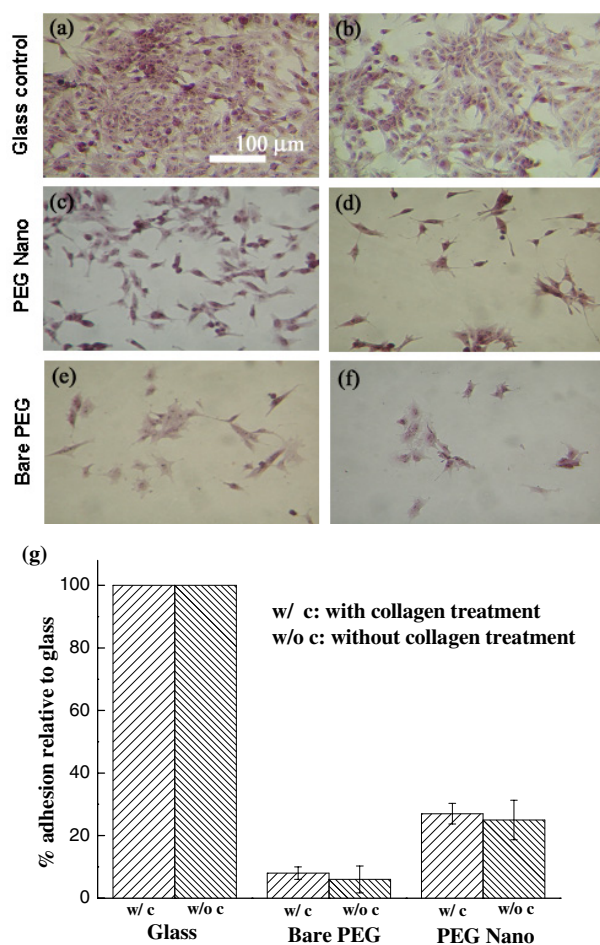


**Figure 6.** Optical micrographs of the stained P19 EC cells adhered on glass, bare PEG, and a PEG nanostructure in the presence of collagen ((a), (c), (e)) and in the absence of collagen ((b), (d), (f)). The cells were cultured for 2 d. Note that the number of adhered cells was increased several times on the nanostructure compared with the bare PEG surface. (g) A summarizing graph for the cell adhesion on the three different surfaces.

formation of focal adhesions was mainly responsible for this behaviour. As shown in figure 7, in these experiments the PEG nanopillars acted as focal sites for fibroblast adhesion. The arrows in the figure indicate the focal sites during the elongation of filopodia and thus the cell growth was guided by the PEG nanopillars. It is noted that surface topography and chemical composition are the cues that are sensed by cells at the time of forming focal adhesions [30]. Thus, a future study would address the exact mechanism of increased cell adhesion as a result of interplay between increased protein adsorption and the guiding role of PEG nanopillars in cell focal adhesion and growth.

## 4. Conclusion

We have developed a simple and fast method for fabricating PEG nanostructures by using the combination of high aspect ratio PUA moulds and UV cross-linkable PEG polymers. In contrast to a thin film of PEG-DMA that was reported earlier, the PEG nanostructures formed using this approach are robust and remain stable upon exposure to solvents like water and

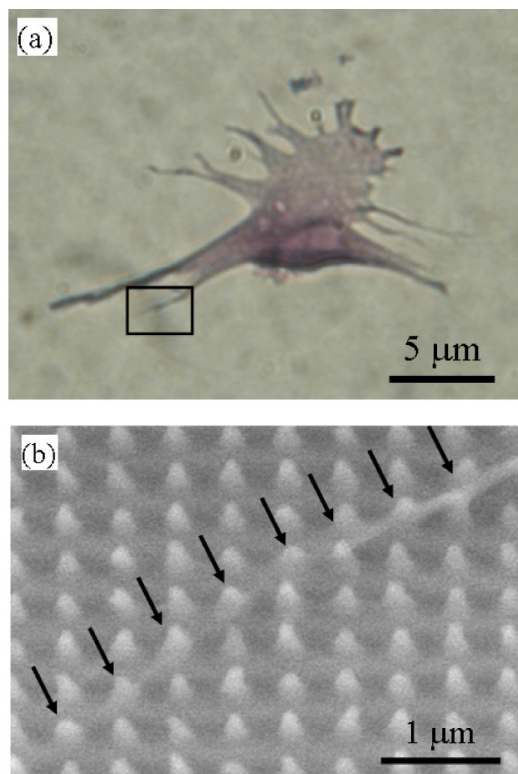


**Figure 7.** Images showing the elongation of filopodia: (a) an optical micrograph of the stained fibroblasts adhered on a PEG nanostructure in the presence of collagen and (b) an ESEM image of a fibroblast attached on PEG nanopillars. The arrows clearly indicate the adhesion sites of the cells along the array of nanopillars.

ethanol for at least two weeks. These nanostructures are hydrophobic due to the capturing of air bubbles, resulting in water contact angles of  $\sim 95^\circ$ . Protein adsorption and cell adhesion on these PEG nanostructures demonstrated that nanostructure modified surfaces were more adhesive compared with bare PEG surface, presumably due to the increased surface area and change of adhesion sites for cells. As with previous reports, PEG nanopillars acted as focal sites for the adhesion of fibroblasts. It is envisioned that our method would be an alternative to construct a PEG patterned surface with good fidelity and reliability, in addition to previous methods such as microcontact printing and photolithography. Also, as PEG-based polymers are frequently used in a broad range of applications in biomaterials science, the control over wettability of the PEG-coated surfaces would provide valuable platforms for fabricating novel biological and biomedical devices.

### Acknowledgments

This work was supported by the Micro Thermal System Research Center of Seoul National University and the

Intelligent Microsystem Program, the 21st Century's Frontier R&D Projects, sponsored by the Korea Ministry of Commerce, Industry and Energy. It was also supported in part by the Ministry of Science and Technology through Bio Tool R&D Project for Cell Research.

### References

- [1] Langer R and Peppas N A 2003 *AIChE J.* **49** 2990
- [2] Langer R and Tirrell D A 2004 *Nature* **428** 487
- [3] Whitesides G M, Ostuni E, Takayama S, Jiang X Y and Ingber D E 2001 *Annu. Rev. Biomed. Eng.* **3** 335
- [4] Mrksich M and Whitesides G M 1996 *Annu. Rev. Biophys. Biomol.* **25** 55
- [5] Mrksich M, Dike L E, Tien J, Ingber D E and Whitesides G M 1997 *Exp. Cell. Res.* **235** 305
- [6] Ostuni E, Kane R, Chen C S, Ingber D E and Whitesides G M 2000 *Langmuir* **16** 7811
- [7] Folch A, Jo B H, Hurtado O, Beebe D J and Toner M 2000 *J. Biomed. Mater. Res.* **52** 346
- [8] Takayama S, McDonald J C, Ostuni E, Liang M N, Kenis P J A, Ismagilov R F and Whitesides G M 1999 *Proc. Natl Acad. Sci. USA* **96** 5545
- [9] Lesho M J and Sheppard N F 1996 *Sensors Actuators B* **37** 61
- [10] Beebe D J, Moore J S, Bauer J M, Yu Q, Liu R H, Devadoss C and Jo B H 2000 *Nature* **404** 588
- [11] Revzin A, Russell R J, Yadavalli V K, Koh W G, Deister C, Hile D D, Mellott M B and Pishko M V 2001 *Langmuir* **17** 5440
- [12] Suh K Y, Seong J, Khademhosseini A, Laibinis P E and Langer R 2004 *Biomaterials* **25** 557
- [13] Suh K Y and Langer R 2003 *Appl. Phys. Lett.* **83** 1668
- [14] Khademhosseini A, Jon S, Suh K Y, Tran T N T, Eng G, Yeh J, Seong J and Langer R 2003 *Adv. Mater.* **15** 1995
- [15] Delamarche E, Schmid H, Michel B and Biebuyck H 1997 *Adv. Mater.* **9** 741
- [16] Bietsch A and Michel B 2000 *J. Appl. Phys.* **88** 4310
- [17] Hui C Y, Jagota A, Lin Y Y and Kramer E J 2002 *Langmuir* **18** 1394
- [18] Kim Y S, Lee H H and Hammond P T 2003 *Nanotechnology* **14** 1140
- [19] Choi S J, Yoo P J, Baek S J, Kim T W and Lee H H 2004 *J. Am. Chem. Soc.* **126** 7744
- [20] Yoo P J, Choi S J, Kim J H, Suh D, Baek S J, Kim T W and Lee H H 2004 *Chem. Mater.* **16** 5000
- [21] Khang D Y and Lee H H 2004 *Langmuir* **20** 2445
- [22] Eppenberger-Eberhardt M, Flamme I, Kurer V and Eppenberger H M 1990 *Dev. Biol.* **139** 269
- [23] Cassie A B D and Baxter S 1944 *Trans. Faraday Soc.* **40** 546
- [24] Adamson A W and Gast A P 1997 *Physical Chemistry of Surfaces* (New York: Wiley)
- [25] Huber D L, Manginell R P, Samara M A, Kim B I and Bunker B C 2003 *Science* **301** 352
- [26] Kuwabara K, Ogino M, Motowaki S and Miyauchi A 2004 *Microelectron. Eng.* **73/74** 752
- [27] Riedel M, Muller B and Wintermantel E 2001 *Biomaterials* **22** 2307
- [28] Dalby M J, Riehle M O, Johnstone H J H, Affrossman S and Curtis A S G 2002 *Tissue Eng.* **8** 1099
- [29] Dalby M J, Riehle M O, Sutherland D S, Agheli H and Curtis A S G 2004 *J. Biomed. Mater. Res. A* **69A** 314
- [30] Vörös J, Blättler T and Textor M 2005 *MRS Bull.* **30** 202